An Efficient Approach to Transmission Line Simulation using Measured or Tabulated S-parameter Data

L. Miguel Silveira Ibrahim M. Elfadel Jacob K. White

Research Laboratory of Electronics and the
Department of Electrical Engineering and Computer Science,
Massachusetts Institute of Technology, Cambridge, MA 02139.

Moni Chilukuri Kenneth S. Kundert

Cadence Design Systems, Inc.
555 River Oaks Parkway, MS 3B1
San Jose, CA 95134

Abstract

In this paper we describe an algorithm for efficient circuit-level simulation of transmission lines which can be specified by tables of frequency-dependent scattering parameters. The approach uses a forced stable section-by-section ℓ_2 minimization approach to construct a high order rational function approximation to the frequency domain data, and then applies guaranteed stable balanced realization techniques to reduce the order of the rational function. The rational function is then incorporated in a circuit simulator using fast recursive convolution. An example of a transmission line with skin-effect is examined to both demonstrate the effectiveness of the approach and to show its generality.

1 Introduction

In the design of communication, high-speed digital, and microwave electronic systems, the behavior of transmission lines formed from packaging and interconnect can have an important impact on system performance. For this reason, including non-ideal transmission lines in circuit simulation has become a topic of much current research [1, 2, 3, 4]. In general, the behavior of stripline and microstrip printed circuit board traces, interchip connections on multichip modules, and coaxial cable connections are most easily represented by frequency-dependent scattering parameters. Since the scattering parameters may be derived from measured data, detailed finite-element simulation, or analytic formulas, a general approach to including transmission lines in circuit simulators is to allow for frequency-dependent elements specified by tables of data.

The most straightforward approach to including general frequency-domain transmission line models in a circuit simulator is to calculate the associated impulse response using an inverse fast Fourier transform [1]. Then, the response of the line at any given time can be determined by convolving the impulse response with an excitation waveform. Such an approach is too computationally expensive for use in general circuit simulation, as it requires that at every simulator timestep, the impulse response be convolved with the entire computed excitation waveform.

An alternative approach is to approximate the frequency-domain representation with a rational function, in which case the associated convolution can be accelerated using a recursive algorithm [2, 3]. Very efficient circuit simulation programs which handle RLCG transmission lines have been developed using such an approach, where the rational function approximation was derived using Padé or moment-matching methods [5, 3, 4].

In this paper we describe a multistage algorithm for efficient circuit simulation of transmission lines which allows general frequency-domain scattering parameter descriptions. First, a decade-by-decade ℓ_2 minimization approach is used to construct a collection of forced stable rational functions whose sum, after a final global ℓ_2 minimization, approximates the original frequency-domain data. This algorithm is described in the next section, and it is observed that the resulting

31st ACM/IEEE Design Automation Conference ®

approximation, though extremely accurate, can have dozens of poles and zeros. Therefore, as described in Section 4, a second step is performed. The unnecessarily high-order model is reduced using a guaranteed stable scheme based on balanced realizations [6, 7]. Once the reduced-order model is derived, it can be combined with the transmission line's inherent delay to generate an impulse response. Then, following what is now a standard approach, the impulse response is efficiently incorporated into the circuit simulator SPICE using recursive convolution. In Section 5, we present results of the time-domain simulation of circuits containing a transmission line with skin-effect.

2 Background

In general, a transmission line can be described in the frequency domain using scattering parameters, in which case

$$\begin{bmatrix} \boldsymbol{Y}_o(j\omega)\boldsymbol{V}_a(j\omega) + \boldsymbol{I}_a(j\omega) \\ \boldsymbol{Y}_o(j\omega)\boldsymbol{V}_b(j\omega) + \boldsymbol{I}_b(j\omega) \end{bmatrix} = \tag{1}$$

$$\begin{bmatrix} 0 & \boldsymbol{S}_{12}(j\omega) \\ \boldsymbol{S}_{12}(j\omega) & 0 \end{bmatrix} \begin{bmatrix} \boldsymbol{Y}_o(j\omega)\boldsymbol{V}_a(j\omega) - \boldsymbol{I}_a(j\omega) \\ \boldsymbol{Y}_o(j\omega)\boldsymbol{V}_b(j\omega) - \boldsymbol{I}_b(j\omega) \end{bmatrix}$$

where $\boldsymbol{V}_a(j\omega), \boldsymbol{I}_a(j\omega)$ and $\boldsymbol{V}_b(j\omega), \boldsymbol{I}_b(j\omega)$ are the voltages and currents at terminals a and b of the transmission line, $\boldsymbol{Y}_o(j\omega)$ is its characteristic admittance, and $\boldsymbol{S}_{12}(j\omega)$ is the relation between the incident and reflected waves on opposite ends of the transmission line. Note, the reason for the unusual choice of $\boldsymbol{Y}_o(j\omega)$ instead of $\boldsymbol{Z}_o(j\omega) = 1/\boldsymbol{Y}_o(j\omega)$ is that for a line with no shunt loss, $\boldsymbol{Z}_o(0) = \infty$.

To incorporate such a general transmission line representation in a circuit simulator, it is necessary to compute the inverse Fourier transforms of $\boldsymbol{S}_{12}(j\omega)$, $\boldsymbol{Y}_o(j\omega)$, and $(\boldsymbol{Y}_o\boldsymbol{S}_{12})(j\omega)$ so as to determine the impulse responses $\boldsymbol{S}_{12}(t), \boldsymbol{Y}_o(t)$, and $(\boldsymbol{Y}_o\boldsymbol{S}_{12})(t)$. Then (1) becomes

$$\begin{aligned} &\boldsymbol{Y}_o(t) \star \boldsymbol{V}_a(t) + \boldsymbol{I}_a(t) = \\ &\qquad (\boldsymbol{Y}_o\boldsymbol{S}_{12})(t) \star \boldsymbol{V}_b(t) - \boldsymbol{S}_{12}(t) \star \boldsymbol{I}_b(t) \end{aligned}$$

$$\begin{aligned} &\boldsymbol{Y}_o(t) \star \boldsymbol{V}_b(t) + \boldsymbol{I}_b(t) = \\ &\qquad (\boldsymbol{Y}_o\boldsymbol{S}_{12})(t) \star \boldsymbol{V}_a(t) - \boldsymbol{S}_{12}(t) \star \boldsymbol{I}_a(t) \end{aligned}$$

where $\star$ is used to denote convolution.

As mentioned in the introduction, if $\boldsymbol{S}_{12}(t), \boldsymbol{Y}_o(t)$ and $(\boldsymbol{Y}_o\boldsymbol{S}_{12})(t)$ are derived by applying the inverse FFT to $\boldsymbol{S}_{12}(j\omega)$, $\boldsymbol{Y}_o(j\omega)$, and $(\boldsymbol{Y}_o\boldsymbol{S}_{12})(j\omega)$ respectively, then the convolutions will be expensive to compute. If, however, $\boldsymbol{S}_{12}(j\omega)$, $\boldsymbol{Y}_o(j\omega)$, and $(\boldsymbol{Y}_o\boldsymbol{S}_{12})(j\omega)$ can be represented using rational function approximations, then the convolution can be performed much faster, and deriving this rational functions is the subject of the subsequent sections. It should be noted that any ideal delay in $\boldsymbol{S}_{12}(j\omega)$ or $(\boldsymbol{Y}_o\boldsymbol{S}_{12})(j\omega)$ must be cancelled before beginning a rational function fitting. This is easily accomplished by multiplying by the associated exponentials [3, 4].

3 Section-by-Section Approximations

The most commonly used approaches to fitting rational functions to frequency domain data are the Padé or moment-matching methods. These methods compute the coefficients of a rational function by matching the function and its derivatives at $s = 0$ and $s = \infty$. If the data available is a table of values measured at certain frequencies, the Padé approach will become less effective, as derivative information at $s = 0$ or $s = \infty$ may be obscured by measurement noise in the table. Below, we take an approach which deals more directly with the frequency-domain data.

3.1 Computing Global Approximants by Weighted ℓ_2 Minimization

One approach to generating a rational function which best matches a frequency response $\boldsymbol{F}(s)$ specified at a set of frequencies $\{s_1, s_2, \cdots, s_m\}$, is to set up and solve, as accurately as possible, the following set of equations:

$$\boldsymbol{H}(s_j) = \boldsymbol{F}(s_j) \qquad j = 1, 2, \cdots, m \tag{2}$$

where

$$\boldsymbol{H}(s) = \frac{\boldsymbol{U}(s)}{\boldsymbol{V}(s)} = \frac{u_q s^q + \cdots + u_1 s + u_0}{v_p s^p + \cdots + v_1 s + 1} \tag{3}$$

is the low-order approximation.

The system in (2) will typically be over-determined. That is, the number of frequency points, m, will exceed the number of unknown coefficients in the approximation, $p + q + 1$, and then (2) can not be satisfied exactly. Instead, consider minimizing the 2-norm of the error, in which case the coefficients of the polynomials $\boldsymbol{U}(s)$ and $\boldsymbol{V}(s)$ are chosen such that

$$\|\boldsymbol{H}(s) - \boldsymbol{F}(s)\|_2 = \|\frac{\boldsymbol{U}(s)}{\boldsymbol{V}(s)} - \boldsymbol{F}(s)\|_2 \tag{4}$$

is minimized for all $s \in \{s_1, s_2, \cdots, s_m\}$. However, this is a nonlinear optimization problem whose solution is difficult to compute. Instead, the problem

can be made linear by weighting the 2-norm by $\boldsymbol{V}(s)$. Then, the minimization problem becomes

$$\min_{\boldsymbol{U},\boldsymbol{V}} \|\boldsymbol{U}(s_j) - \boldsymbol{V}(s_j)\boldsymbol{F}(s_j)\|_2 \qquad j = 1, \cdots, m. \quad (5)$$

Minimizing this weighted 2-norm does not guarantee that the resulting rational function will be accurate at any particular frequency, and this is unacceptable for use in circuit simulation. In order to insure that the steady-state will be computed exactly, the ℓ_2 minimization must be constrained as follows:

$$\begin{cases} \frac{\boldsymbol{U}_{(0)}}{\boldsymbol{V}_{(0)}} = \boldsymbol{F}(0) \\ min_{\boldsymbol{U},\boldsymbol{V}} \|\boldsymbol{U}(s_j) - \boldsymbol{V}(s_j)\boldsymbol{F}(s_j)\|_2 \qquad j = 1, \cdots, m \\ \lim_{s\to\infty} \frac{\boldsymbol{U}_{(s)}}{\boldsymbol{V}_{(s)}} = \lim_{s\to\infty} \boldsymbol{F}(s). \end{cases} \quad (6)$$

The above constrained ℓ_2-minimization procedure can still produce poor results if the frequency range is more than a few decades. One of the difficulties is that the weighting introduced to generate the linear problem in (6) substantially favors high frequencies. This results in a rational function approximant which is very accurate at the high frequencies but inaccurate in the low frequency range. A second difficultly is that the minimization becomes ill-conditioned if the frequency range is more than a few decades. This is easily understood by examining the structure of the matrix obtained from the minimization portion of (6). Each row of this matrix corresponds to computing $\boldsymbol{U}(s_j) - \boldsymbol{V}(s_j)\boldsymbol{F}(s_j)$ at some frequency value s_j. Therefore, the entries along each row of the matrix are powers of the corresponding frequency value. This implies that if the span of frequencies is large, then the magnitude of the entries on rows associated with high frequencies will be much larger than those in rows corresponding to low frequency values. Not only may this cause overflow in the computation, but also results in an extremely ill-conditioned matrix.

3.2 Computing Section-by-Section Approximants

In order to avoid the numerical ill-conditioning and the uneven frequency weighting, it is desirable to limit the frequency range for the ℓ_2 minimization. The idea of computing local approximations leads to a **sectioning** algorithm in which only accurate local approximations are computed. The remaining problem is how to incorporate all the local information resulting from the various approximations into a global approximant.

Algorithm 1 (Section-by-Section Approx.)

```
Eliminate ideal delay.
Partition frequency range into
  sections Ω_1, ..., Ω_M with associated
  frequencies {w_i1, ..., w_im_Ω_i},
  i = 1, ..., M.
for (k = 1; k <= M; k++) {
   subtract previous approximants
     F_k(w_k,j) = F(w_k,j) - Σ_{l=1}^{k-1} H_l(jw_k,j)
   Fit H_k(s) to F_k(w_i,j).
   Delete unstable poles in H_k(s).
}
```

Our approach is to perform the local approximations in a repeated fashion. Initially, the frequency range of interest, $\boldsymbol{\Omega} = [w_{min}, w_{max}]$, is partitioned into small sections, $\boldsymbol{\Omega}_1, \boldsymbol{\Omega}_2, \cdots, \boldsymbol{\Omega}_M$, such that $\boldsymbol{\Omega} = \bigcup_{i=1}^{M} \boldsymbol{\Omega}_i$, where each $\boldsymbol{\Omega}_i$ is a decade or two long. Then, starting with the lowest frequency range $\boldsymbol{\Omega}_1$, with frequency values $\boldsymbol{F}(w_{11}), \boldsymbol{F}(w_{12}), \cdots, \boldsymbol{F}(w_{1m})$, a constrained ℓ_2 minimization is performed and a local approximant is computed. Once the first local approximation, $\tilde{\boldsymbol{H}}_1(s)$, is obtained in the form of a collection of poles and their corresponding residues, it is examined and the stable poles are retained while the unstable ones are discarded. This results in a *forced stable* approximation, $\boldsymbol{H}_1(s)$. Next, in the second section $\boldsymbol{\Omega}_2$, the values $\boldsymbol{F}(w_{21}) - \boldsymbol{H}_1(w_{21}), \boldsymbol{F}(w_{22}) - \boldsymbol{H}_1(w_{22}), \cdots, \boldsymbol{F}(w_{2m}) - \boldsymbol{H}_1(w_{2m})$ are fit with $H_2(s)$, using the constrained weighted ℓ_2 minimization. The result of the second fit is an improved approximation, $\boldsymbol{H}_1(s) + \boldsymbol{H}_2(s) \approx \boldsymbol{F}(s)$. The procedure is repeated until data in the last frequency section, $\boldsymbol{\Omega}_M$, is approximated. A simplified form of this sectioning algorithm is shown in pseudo-code form as Algorithm 1.

It should be noted that this iterative section-by-section algorithm computes approximations which match successively higher frequency ranges. However, when subtracting the already computed approximations from the exact data, some erroneous dynamics may be introduced at lower frequencies. Therefore, a final constrained global ℓ_2 minimization is performed in which the computed poles are used and the residues recalculated.

4 Model-Order Reduction by Truncated Balanced Realization

The frequency-domain data fitting method described in the previous section generates a stable transfer function $\boldsymbol{H}(s)$, but generally the function will have a large number of poles. Since the computational cost of including transfer functions in circuit simulation is proportional to the number of poles, these transfer functions will be computationally expensive. To improve the efficiency, we use a model-order reduction approach which has three main steps. First, a well-conditioned state-space realization of $H(s)$ is formed. Second, the state-space realization is *balanced*. Third, the balanced realization is truncated. Using this type of balanced realization approach has a key advantage. The resulting simplified $\boldsymbol{H}_r(s)$ is *guaranteed* stable if $\boldsymbol{H}(s)$ is stable.

4.1 State-Space Realization

To reduce the order of the transmission line model derived in the previous section, first we consider its state-space representation

$$\begin{aligned} \dot{\boldsymbol{x}} &= \boldsymbol{A}\boldsymbol{x} + \boldsymbol{B}u, & \boldsymbol{x}, \boldsymbol{B} \in \mathbb{R}^n,\ u \in \mathbb{R},\ \boldsymbol{A} \in \mathbb{R}^{n\times n} \\ y &= \boldsymbol{C}\boldsymbol{x}, & y \in \mathbb{R}, \boldsymbol{C} \in \mathbb{R}^n \end{aligned} \tag{7}$$

such that $\boldsymbol{H}(s) = \boldsymbol{C}(s\boldsymbol{I} - \boldsymbol{A})^{-1}\boldsymbol{B}$.

Converting $\boldsymbol{H}(s)$ in a pole-residual form to a state-space form is a standard problem, and it is tempting to use one of the common techniques (canonical controllability realization, canonical observability realization, etc.) to find the matrices $\boldsymbol{A}$, $\boldsymbol{B}$, and $\boldsymbol{C}$. However, these approaches can result in a system matrix $\boldsymbol{A}$ which is poorly scaled and therefore unsuitable for computations.

Instead, when all the poles are simple and real, the matrix $\boldsymbol{A}$ can be chosen equal to a diagonal matrix where the real poles are the diagonal coefficients. The control and observation matrices $\boldsymbol{B}$ and $\boldsymbol{C}$ can then be chosen based on the residues of the poles. More explicitly, given

$$\boldsymbol{H}(s) = \sum_{k=1}^{n} \frac{r_k}{s - p_k} \tag{8}$$

where all the poles are negative reals and all the residues are real,

$$\begin{aligned} \boldsymbol{A} &= diag(p_1, \ldots, p_n) \\ \boldsymbol{B} &= (\sqrt{|r_1|}, \ldots, \sqrt{|r_n|})^T \\ \boldsymbol{C} &= (\mathrm{sign}(r_1)\sqrt{|r_1|}, \ldots, \mathrm{sign}(r_n)\sqrt{|r_n|}) \end{aligned}$$

When $\boldsymbol{H}(s)$ has pairs of complex conjugate poles, a block diagonal matrix $\boldsymbol{A}$ can be constructed where the blocks are all 2×2 and correspond to pairing the complex conjugate poles in state-space realizations of order 2. It is also possible to find suitable state-space realizations when some of the poles are repeated. For transmission line examples there are only real, simple poles, and therefore the purely diagonal realization can be used.

4.2 Balanced Realizations

Once the state-space representation is adopted, it has to be internally balanced [6]. That is, given $\boldsymbol{H}(s) = \boldsymbol{C}(s\boldsymbol{I} - \boldsymbol{A})^{-1}\boldsymbol{B}$, the choice of the triplet $[\boldsymbol{A}, \boldsymbol{B}, \boldsymbol{C}]$ is not unique. Indeed, a linear coordinate transformation $\tilde{\boldsymbol{x}} = \boldsymbol{T}\boldsymbol{x}$ modifies the triplet $[\boldsymbol{A}, \boldsymbol{B}, \boldsymbol{C}]$ to $[\tilde{\boldsymbol{A}}, \tilde{\boldsymbol{B}}, \tilde{\boldsymbol{C}}]$ *without* modifying $\boldsymbol{H}(s)$.

For the specific purpose of extracting *stable* reduced-order models from the state-space representation, it is desirable that the new triplet $[\tilde{\boldsymbol{A}}, \tilde{\boldsymbol{B}}, \tilde{\boldsymbol{C}}]$ be in a form that allows such an extraction using some simple operation on the new state $\tilde{\boldsymbol{x}} = \boldsymbol{T}\boldsymbol{x}$. The easiest conceivable such operation would be simple state truncation. Moore has shown [6] that such a transformation exists and he called the corresponding triplet $[\tilde{\boldsymbol{A}}, \tilde{\boldsymbol{B}}, \tilde{\boldsymbol{C}}]$ a *balanced realization* of the transfer function $\boldsymbol{H}(s)$. The word "balanced" refers to the fact that the controllability and observability gramians of the triplet $[\tilde{\boldsymbol{A}}, \tilde{\boldsymbol{B}}, \tilde{\boldsymbol{C}}]$ are both equal to the *same* diagonal matrix. The balancing transformation $\boldsymbol{T}$ can be computed explicitly for any triplet $[\boldsymbol{A}, \boldsymbol{B}, \boldsymbol{C}]$, and in particular for the diagonal realization that we have proposed in the previous paragraph. The numerical cost of such a computation is that of solving two matrix Lyapunov equations to obtain the controllability and observability gramians, and one symmetric eigenvalue problem to diagonalize their product.

4.3 Truncated Realization

The triplet $[\tilde{\boldsymbol{A}}, \tilde{\boldsymbol{B}}, \tilde{\boldsymbol{C}}]$ obtained by applying the balancing transformation $\boldsymbol{T}$ to the triplet $[\boldsymbol{A}, \boldsymbol{B}, \boldsymbol{C}]$ has the property that simple reordering and truncation of the state vector $\tilde{\boldsymbol{x}}$ with the corresponding reordering of the system matrices *necessarily* produce *stable* reduced-order models at any desirable order. Let k be this order, and let $[\tilde{\boldsymbol{A}}_k, \tilde{\boldsymbol{B}}_k, \tilde{\boldsymbol{C}}_k]$ be the reduced-order model with a transfer function $\boldsymbol{H}_k(s)$. It can then be shown [6, 7] that the error transfer function

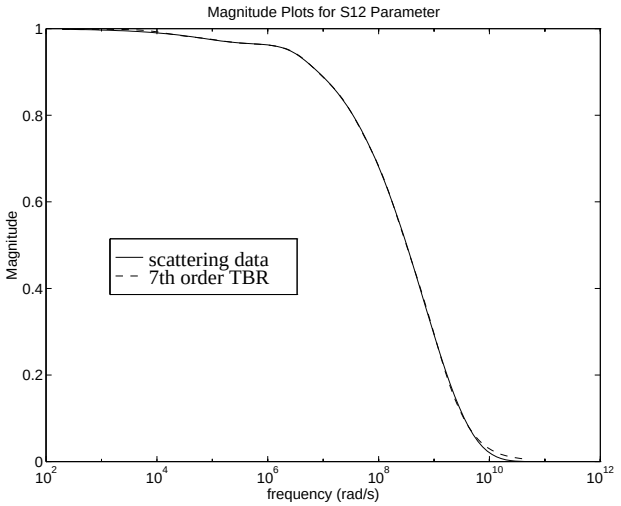

Figure 1: Accuracy of the reduced-order model fit for the magnitude of the $\boldsymbol{S}_{12}$ transfer function with respect to the transmission line data points.

$\boldsymbol{E}_k(s) = \boldsymbol{H}(s) - \boldsymbol{H}_k(s)$ has an L_∞ norm which consistently decreases to zero as k is increases. This L_∞ norm corresponds to the peak of the magnitude of $E_k(s)$. Note that Padé approximation methods [5] do not enjoy such an error reduction property.

The above approach, combined with an a posteriori least-squares/collocation technique to insure an exact match at zero frequency, produces low order models which are stable, have a small number of poles, and match well at all frequencies. To show this, consider the example of matching $\boldsymbol{S}_{12}(\boldsymbol{j}\omega)$ in a transmission line where skin effects are significant (Figure 1). In this case, the section-by-section algorithm created a 21 pole approximation, but it was found that reduced order model with seven poles accurately approximated the transfer function. As Figure 1 shows, the match between the reduced-order model and the transmission line data is well within 1%.

5 Experimental Results

In this Section, we present results from an implementation of the above algorithm based on a modified version of SPICE3 [8]. We first show that the reduced order model produces nearly the same time-domain waveforms as the more complete sectioning based model, but with many fewer poles. Second, we show an example with realistic transistor drivers and receivers, to demonstrate the ability of the method to simulate complete circuit descriptions. Note, a comparison to the more commonly used FFT methods

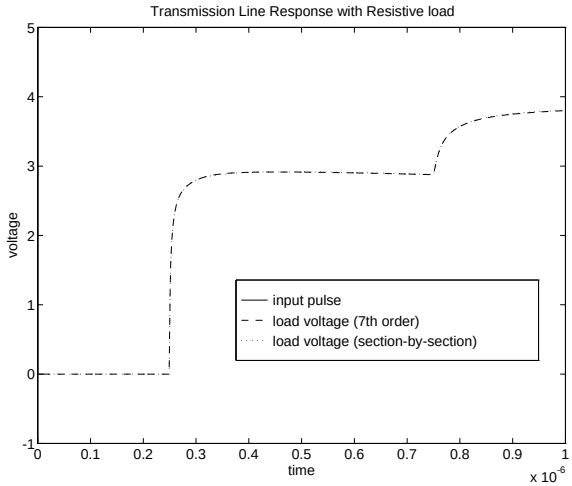

Figure 2: Time response obtained from applying a pulse to a resistively terminated transmission line. The figure shows the response of a line modeled with a 7 pole reduced-order model and that of a line modeled with the approximation resulting from our sectioning algorithm, which has more than 20 poles.

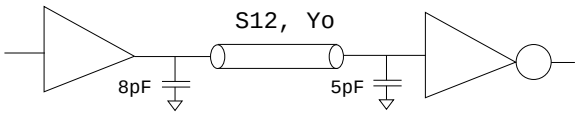

Figure 3: CMOS driver and load connected by a transmission line with skin-effect.

was not included, recursive convolution has previously been shown to be both more accurate and much more efficient[3].

In Figure 2 we present the time-domain results of applying a 5 volt step to a 50Ω terminated transmission line with significant skin-effect. In the figure, we compare the time response of the 7-th order reduced-order model with the time response obtained using the full sectioning based approximant, which has more than twenty poles. The fact that the two responses are indistinguishable in the figure shows that an excellent match has been obtained. And since the cost of recursive convolution is proportional to the number of poles in the reduced-order model, the 7-th order model is nearly three times more efficient.

In Figure 4 we present the time-domain results obtained from the circuit in Figure 3, where the transmission line is the one from the previous example. The driver and the load are both CMOS inverters, where the transistors are described using SPICE3's default level 2 model with $W/L = 750$ for the p-type pullup devices and $W/L = 400$ for the n-type pull-down devices. The simulation results show clearly that the

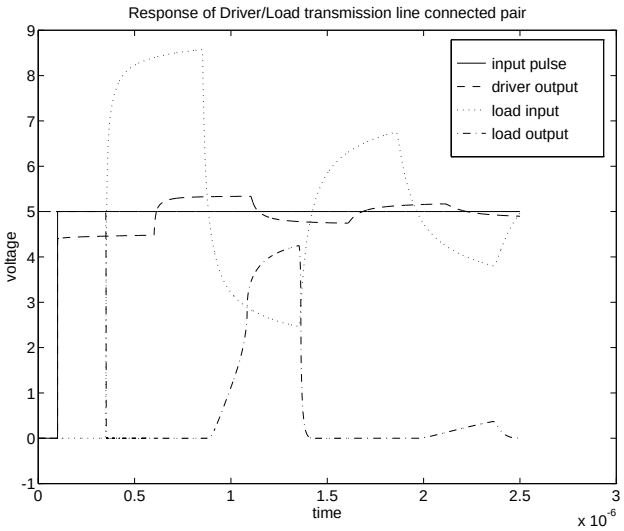

Figure 4: Time response obtained from a nonlinear circuit with a transmission connecting driver and load. The transmission line is modeled with a 7 pole reduced-order model.

improper line termination causes reflections to transmit back and forth on the line and falsely trigger the load inverter.

6 Conclusions and Acknowledgements

In this paper we presented a robust and efficient multistage algorithm for including general transmission lines, described by frequency-domain data, in a circuit simulation program. The algorithm constructs a rational function fit to the frequency-domain data using a section-by-section least-squares fitting procedure followed by model-order reduction based on balanced realizations. Then, the resulting rational transfer function can be incorporated in a circuit simulator using recursive convolution. Numerical experiments were presented for a transmission line problem with skin-effects to show that frequency and time-domain responses could be accurately computed.

It should be noted that the procedure described above is quite general, and could be used to incorporate and frequency-dependent element in a circuit simulator, not just transmission lines.

This work was supported by the Advanced Research Projects Agency contract N00014-91-J-1698, the National Science Foundation contract (MIP-8858764 A02) and (9117724-MIP), the Portuguese "Junta Nacional de Investigação Científica e Tecnológica" under project "Ciência", an I.B.M. fellowship and a grant from Digital Equipment Corporation.

References

[1] J. E. Schutt-Aine and R. Mittra. Scattering Parameter Transient Analysis of Transmissions Lines loaded with Nonlinear Terminations. *IEEE Transactions on Microwave Theory and Techniques*, MTT-36:529–536, 1988.

[2] C. Gordon, T. Blazeck, and R. Mittra. Time-domain simulation of multiconductor transmission lines with frequency-dependent losses. *IEEE Trans. CAD*, 11(11):1372–1387, November 1992.

[3] Shen Lin and Ernest S. Kuh. Transient Simulation of Lossy Interconnects Based on the Recursive Convolution Formulation. *IEEE Trans. Circuits Syst.*, 39(11):879–892, November 1992.

[4] J. E. Bracken, V. Raghavan, and R. A. Rohrer. Interconnect Simulation with Asymptotic Waveform Evaluation. *IEEE Trans. Circuits Syst.*, 39(11):869–878, November 1992.

[5] Lawrence T. Pillage, Xiaoli Huang, and Ronald A. Rohrer. AWEsim: Asymptotic Waveform Evaluation for Timing Analysis. In 26^{th} *ACM/IEEE Design Automation Conference*, pages 634–637, Las Vegas, Nevada, June 1989.

[6] Bruce Moore. Principal Component Analysis in Linear Systems: Controllability, Observability, and Model Reduction. *IEEE Transactions on Automatic Control*, AC-26(1):17–32, February 1981.

[7] Keith Glover. All optimal Hankel-norm approximations of linear multivariable systems and their l^{∞}-error bounds. *International Journal on Control*, 39(6):1115–1193, June 1984.

[8] Thomas L. Quarles. The SPICE3 Iimplementation Guide. Technical Report ERL M89/44, Electronics Research Laboratory Report, University of California, Berkeley, Berkeley, California, April 1989.